2-17-2009

Global Aspects of the Scalar Meson Puzzle

Joseph Schechter
Department of Physics, Syracuse University, Syracuse, NY

Amir H. Fariborz
State University of New York Institute of Technology

Renata Jora
INFN Roma

SU-4252-875

Global aspects of the scalar meson puzzle

Amir H. Fariborz [a] ‡, Renata Jora [b] †, and Joseph Schechter [c] §
[a] *Department of Mathematics/Science, State University of New York Institute of Technology, Utica, NY 13504-3050, USA.*
[b] *INFN Roma, Piazzale A Moro 2, Roma, I-00185 Italy. and*
[c] *Department of Physics, Syracuse University, Syracuse, NY 13244-1130, USA,*
(Dated: February 17, 2009)

A generalized linear sigma model for low energy QCD is employed to study the quark structure of eight low lying scalar isomultiplets as well as eight low lying pseudoscalar isomultiplets. The model, building on earlier work, assumes the possible mixing of quark anti-quark states with others made of two quarks and two antiquarks. No *a priori* assumption is made about the quark contents of the states, which emerge as predictions. An amusing and contrasting pattern for the quark structure is found; the lighter conventional pseudoscalars are, as expected, primarily of two quark type whereas the lighter scalars have very large four quark admixtures. The new feature of the present paper compared to earlier ones in this series involves the somewhat subtle and complicated effects of SU(3) flavor breaking. They do not alter the general pattern of two quark vs. four quark mixing obtained in the SU(3)symmetric case but, of course, give a more detailed picture.

PACS numbers: 13.75.Lb, 11.15.Pg, 11.80.Et, 12.39.Fe

I. INTRODUCTION

Although it is an ancient subject, the study of light scalar mesons has greatly intensified in the last generation. Some representative earlier works of this period are given in [1]-[19].

The "global" aspect of the scalar puzzle is the unusual spectroscopy of the light scalar nonet. At present, the scalars below 1 GeV appear to fit into a nonet as:

$$\begin{aligned} I=0: m[f_0(600)] &\approx 500 \text{ MeV} \\ I=1/2: \quad m[\kappa] &\approx 800 \text{ MeV} \\ I=0: m[f_0(980)] &\approx 980 \text{ MeV} \\ I=1: m[a_0(980)] &\approx 980 \text{ MeV} \end{aligned} \tag{1}$$

This level ordering is seen to be flipped compared to that of the standard vector meson nonet:

$$\begin{aligned} I=1: m[\rho(776)] &\approx 776 \text{ MeV} \quad n\bar{n} \\ I=0: m[\omega(783)] &\approx 783 \text{ MeV} \quad n\bar{n} \\ I=1/2: m[K^*(892)] &\approx 892 \text{ MeV} \quad n\bar{s} \\ I=0: m[\phi(1020)] &\approx 1020 \text{ MeV} \quad s\bar{s} \end{aligned} \tag{2}$$

Here the standard quark content (n stands for a non-strange quark while s stands for a strange quark) is displayed at the end for each case. The vector mass ordering is seen to just correspond to the number of s-type quarks in each state. It was pointed out a long time ago in Ref. [20], that the level order is automatically flipped when mesons are made of two quarks and two antiquarks instead of a single quark and antiquark. That argument was given for a diquark- anti diquark structure but is easily seen to also hold for a meson-meson "molecule" type structure which was advocated, at least for a partial nonet, in Ref. [21]. Note that, in the "ideal" four quark picture, the states in Eq.(1) consecutively have the quark contents: $nn\bar{n}\bar{n}$, $nn\bar{n}\bar{s}$, $ns\bar{n}\bar{s}$ and $ns\bar{n}\bar{s}$. One also notes that the masses of the putative scalar nonet are significantly lower than the other (tensor and two axial vector) p-wave quark-antiquark nonets. There are enough other scalar candidates [$a_0(1450)$, $K_0(1430)$ and two of $f_0(1370)$, $f_0(1500,)$ $f_0(1710)$] to make another nonet although the masses of its contents seem somewhat higher than an expected scalar p-wave nonet. Based on the usual effect that two mixing levels repel as well as some more detailed features, it was suggested [22] that a global picture

‡ Email: fariboa@sunyit.edu
† Email: cjora@physics.syr.edu
§ Email: schechte@physics.syr.edu

of these scalars might consist of a lighter "four quark" nonet mixing with a heavier "two quark" nonet. Further work in this direction has been presented by a number of authors [23]-[26].

A field theoretic toy model to study these features was introduced in [28]. Although simple in conception it turned out to be rather complicated to implement; as a result the present authors examined its features in further detail in [29, 30, 31, 32, 33]. While the general treatment in [29] only used the tree level Ward-type identities of the theory, the treatments in [30] and [31] employed specific potential terms chosen in a systematic way to correspond to terms with the minimum number of underlying quark lines. Furthermore the quark mass terms were neglected, which not only is a simplifying feature but is also a check that the peculiar mixing results found are not an artifice of a particular choice of symmetry breaking terms. (In QCD it is expected that the main features of the various particle multiplets should also hold in the limit of zero light quark masses.) Next, in [32] it was demonstrated that the results did not change much when the minimal mass term was included with equal masses for all three light quarks. It was also shown that the current algebra theorem [34] for pion pion scattering holds to a very good approximation in this more complicated case where the ordinary pion has a small admixture of a state containing two quarks and two antiquarks. The theorem has a very small correction due to a very small violation of the partially conserved axial vector current hypothesis in the model, however. Most recently, in [33] an amusing connection between the model and the instanton approach to QCD dynamics was discussed. This connection is not so surprising when one notices that it is the (broken by instantons) $U(1)_A$ symmetry which formally distinguishes the "four quark" from the "two quark" meson states.

In the present paper we include the flavor SU(3) symmetry breaking in the model. As will be seen, this is not a very simple matter, even in the tree approximation being used. Within this framework we will not introduce any further approximations in our numerical treatment. Furthermore, the sensitivity of the predictions to the main uncertainties in the experimental inputs will be explicitly displayed.

Considering the relatively large number of "outputs," it may be desirable to immediately just display our main "typical" results. These are the masses and the "two quark" vs. "four quark" percentages of the members of all four nonets (light and heavy pseudoscalars and light and heavy scalars). They are listed in Tables I and II. Isospin but not SU(3) symmetry is being assumed. Note that for the I=1/2 and I=1 states, the prime denotes the heavier particle. For the I=0 particles there are four states of each parity and they are denoted by subscripts 1, 2, 3, 4 in order of increasing mass. Altogether, considering the isospin degeneracy, there are 16 different masses. The 8 inputs comprise the pion decay constant, the four masses: [m_π, $m_{\pi'}$, m_a, m'_a], the strange to non strange quark mass ratio (which is related to assuming a value for m_K) and (as to be explained later) the sum and the product of all the four I=0 pseudoscalar squared masses for each of the possible scenarios for their identification with experimental states.

Thus there are 9 mass predictions and 16 predictions for the two-quark and four quark percentages being displayed in Tables I and II. To compare with Eq.(1) for the "experimental" light scalar nonet, we read off the mass pattern:

$$f_1(742),\ \kappa(1067),\ a(980)\ f_2(1085), \tag{3}$$

in which only the $a(980)$ mass was an input. Clearly, the pattern, featuring an approximate degeneracy of one I=0 state and the I=1 state together with a flipping compared to the standard vector meson order, is very similar to the experimental one in Eq.(1). Actually, these "tree level" predictions are expected to receive some non-trivial corrections as to be discussed later. We also read from Table II that the light scalar nonet is predicted to be predominantly of 4-quark type. On the other hand, the heavy scalar nonet is predicted to be predominantly of 2-quark type and to have the standard (vector meson like) pattern:

$$a'(1474),\ f_3(1493),\ \kappa'(1624),\ f_4(1784). \tag{4}$$

The conventional light pseudoscalar nonet is read from Table I as,

$$\pi(137),\ K(515),\ \eta_1(553),\ \eta_2(982), \tag{5}$$

where the structure is clearly close to the conventional one. Notice the well known fact that this nonet agrees in ordering with that of the standard vector nonet in the sense that the I=1 state is lightest but disagrees in that the lighter I=0 state is not at all close to the I=1 state. At the theoretical level, this arises from axial U(1) (instanton type) terms as are included here. It can also be read off that the light pseudoscalar nonet members are predicted to be predominantly of "2-quark", i.e. $\bar{q}q$, type. In contrast, the heavy pseudoscalar nonet members are predicted to be of predominantly "4-quark" type with a similar mass ordering as the light pseudoscalars; namely,

$$\pi'(1215),\ K'(1195),\ \eta_3(1225),\ \eta_4(1784). \tag{6}$$

In this multiplet, the distortion of the pattern from that of the standard vector multiplet seems to reflect the greater role of "instanton" effects over "4-quark" effects.

A detailed discussion of how these results were obtained is given in the following sections. Section II briefly summarizes the "toy Lagrangian" and the choice of input parameters. The needed mass matrices are presented in section III and Appendix B. The first part of Section IV and, especially, Appendix A explain in a step by step way how the Lagrangian parameters (other than those associated with the "instanton" terms) are related to the experimental data. The second part of section IV explains predictions of the model and their sensitivity to changes in the input parameters. Section V explains the work associated with the instanton terms and the complicated I=0 pseudoscalar sector. Finally, conclusions and some further discussion are presented in section VI.

State	$\bar{q}q$%	$\bar{q}\bar{q}qq$%	m (GeV)
π	85	15	0.137
π'	15	85	1.215
K	86	14	0.515
K'	14	86	1.195
η_1	89	11	0.553
η_2	78	22	0.982
η_3	32	68	1.225
η_4	1	99	1.794

TABLE I: Typical predicted properties of pseudoscalar states: $\bar{q}q$ percentage (2nd column), $\bar{q}\bar{q}qq$ (3rd column) and masses (last column).

State	$\bar{q}q$%	$\bar{q}\bar{q}qq$%	m (GeV)
a	24	76	0.984
a'	76	24	1.474
κ	8	92	1.067
κ'	92	8	1.624
f_1	40	60	0.742
f_2	5	95	1.085
f_3	63	37	1.493
f_4	93	7	1.783

TABLE II: Typical predicted properties of scalar states: $\bar{q}q$ percentage (2nd column), $\bar{q}\bar{q}qq$ (3rd column) and masses (last column).

II. MODEL LAGRANGIAN AND PHYSICAL INPUTS

The model employs the 3×3 matrix chiral nonet fields:

$$M = S + i\phi, \qquad\qquad M' = S' + i\phi'. \tag{7}$$

The matrices M and M' transform in the same way under chiral SU(3) × SU(3) transformations but may be distinguished by their different $U(1)_A$ transformation properties. M describes the "bare" quark antiquark scalar and pseudoscalar nonet fields while M' describes "bare" scalar and pseudoscalar fields containing two quarks and two antiquarks. At the symmetry level with which we are working, it is unnecessary to further specify the four quark field configuration. The four quark field may, most generally, be imagined as some linear combination of a diquark-antidiquark and a "molecule" made of two quark-antiquark "atoms".

The general Lagrangian density which defines our model is

$$\mathcal{L} = -\frac{1}{2}\mathrm{Tr}\left(\partial_\mu M \partial_\mu M^\dagger\right) - \frac{1}{2}\mathrm{Tr}\left(\partial_\mu M' \partial_\mu M'^\dagger\right) - V_0\left(M, M'\right) - V_{SB}, \tag{8}$$

where $V_0(M, M')$ stands for a function made from $\mathrm{SU(3)_L}\times\ \mathrm{SU(3)_R}$ (but not necessarily $\mathrm{U(1)_A}$) invariants formed out of M and M'.

As we previously discussed [30], the leading choice of terms corresponding to eight or fewer quark plus antiquark lines at each effective vertex reads:

$$\begin{aligned} V_0 = & - c_2\,\mathrm{Tr}(MM^\dagger) + c_4^a\,\mathrm{Tr}(MM^\dagger MM^\dagger) \\ & + d_2\,\mathrm{Tr}(M'M'^\dagger) + e_3^a(\epsilon_{abc}\epsilon^{def}M_d^aM_e^bM_f'^c + h.c.) \\ & + c_3\left[\gamma_1 \ln(\frac{\det M}{\det M^\dagger}) + (1-\gamma_1)\ln\frac{\mathrm{Tr}(MM'^\dagger)}{\mathrm{Tr}(M'M^\dagger)}\right]^2 . \end{aligned} \tag{9}$$

All the terms except the last two have been chosen to also possess the $\mathrm{U(1)_A}$ invariance. The symmetry breaking term which models the QCD mass term takes the form:

$$V_{SB} = -2\,\mathrm{Tr}(A\,S) \tag{10}$$

where $A = diag(A_1, A_2, A_3)$ are proportional to the three light quark masses. The model allows for two-quark condensates, $\alpha_a = \langle S_a^a\rangle$ as well as four-quark condensates $\beta_a = \langle S'^a_a\rangle$. Here we assume [35] isotopic spin symmetry so $\mathrm{A_1} = \mathrm{A_2}$ and:

$$\alpha_1 = \alpha_2 \neq \alpha_3, \qquad\qquad \beta_1 = \beta_2 \neq \beta_3 \tag{11}$$

We also need the "minimum" conditions,

$$\left\langle \frac{\partial V_0}{\partial S}\right\rangle + \left\langle \frac{\partial V_{SB}}{\partial S}\right\rangle = 0, \qquad \left\langle \frac{\partial V_0}{\partial S'}\right\rangle = 0. \tag{12}$$

There are twelve parameters describing the Lagrangian and the vacuum. These include the six coupling constants given in Eq.(9), the two quark mass parameters, $(A_1 = A_2, A_3)$ and the four vacuum parameters $(\alpha_1 = \alpha_2, \alpha_3, \beta_1 = \beta_2, \beta_3)$.The four minimum equations reduce the number of needed input parameters to eight.

Five of these eight are supplied by the following masses together with the pion decay constant:

$$\begin{aligned} m[a_0(980)] &= 984.7 \pm 1.2\,\mathrm{MeV} \\ m[a_0(1450)] &= 1474 \pm 19\,\mathrm{MeV} \\ m[\pi(1300)] &= 1300 \pm 100\,\mathrm{MeV} \\ m_\pi &= 137\,\mathrm{MeV} \\ F_\pi &= 131\,\mathrm{MeV} \end{aligned} \tag{13}$$

Because $m[\pi(1300)]$ has such a large uncertainty, we will, as previously, examine predictions depending on the choice of this mass within its experimental range. The sixth input will be taken as the light "quark mass ratio" A_3/A_1, which will be varied over an appropriate range. The remaining two inputs will be taken from the masses of the four (mixing) isoscalar, pseudoscalar mesons. This mixing is characterized by a 4×4 matrix M_η^2. A practically convenient choice is to consider $\mathrm{Tr}M_\eta^2$ and $\det M_\eta^2$ as the inputs.

Given these inputs there are a very large number of predictions. At the level of the quadratic terms in the Lagrangian, we predict all the remaining masses and decay constants as well as the angles describing the mixing between each of (π, π'), (K, K'), (a_0, a_0'), (κ, κ') multiplets and each of the 4×4 isosinglet mixing matrices (each formally described by six angles).

Defining the total potential $V = V_0 + V_{SB}$, the four minimum conditions explicitly read:

$$\left\langle \frac{\partial\, V}{\partial\, S_1^1}\right\rangle = 4\,e_3^a\,\alpha_1\,\beta_3 + 4\,e_3^a\,\beta_1\,\alpha_3 - 2\,c_2\,\alpha_1 + 4\,c_4^a\,\alpha_1^3 - 2\,A_1 = 0. \tag{14}$$

$$\left\langle \frac{\partial\, V}{\partial\, S_3^3}\right\rangle = 8\,e_3^a\,\beta_1\,\alpha_1 - 2\,c_2\,\alpha_3 + 4\,c_4^a\,\alpha_3^3 - 2\,A_3 = 0. \tag{15}$$

$$\left\langle \frac{\partial\, V}{\partial\, S'^1_1}\right\rangle = 4\,e_3^a\,\alpha_1\,\alpha_3 + 2\,d_2\,\beta_1 = 0. \tag{16}$$

$$\left\langle \frac{\partial\, V}{\partial\, S'^3_3}\right\rangle = 4\,e_3^a\,\alpha_1^2 + 2\,d_2\,\beta_3 = 0. \tag{17}$$

III. MASS MATRICES

In order to evaluate the eight independent parameters from experiment it is necessary to first obtain the formulas for the squared mass matrices corresponding to each set of particles with the same parity and isotopic spin quantum numbers. These are calculated by taking the second derivatives of the potential with respect to the appropriate fields.

For the two mixing "pion" states (I=1, P=−) we find:

$$\left(M_\pi^2\right) = \begin{bmatrix} 4\,e_3^a\,\beta_3 - 2\,c_2 + 4\,c_4^a\,\alpha_1^2 & 4\,e_3^a\,\alpha_3 \\ 4\,e_3^a\,\alpha_3 & 2\,d_2 \end{bmatrix} \tag{18}$$

The 2 × 2 K meson matrix (I=1/2, P=−) reads:

$$\left(M_K^2\right) = \begin{bmatrix} 4\,e_3^a\,\beta_1 - 2\,c_2 + 4\,c_4^a\,\alpha_1^2 - 4\,c_4^a\,\alpha_1\,\alpha_3 + 4\,c_4^a\,\alpha_3^2 & 4\,e_3^a\,\alpha_1 \\ 4\,e_3^a\,\alpha_1 & 2\,d_2 \end{bmatrix} \tag{19}$$

In the case of the two scalar a-mesons (I=1, P=+) the mass squared mixing matrix reads:

$$\left(X_a^2\right) = \begin{bmatrix} -4\,e_3^a\,\beta_3 - 2\,c_2 + 12\,c_4\,\alpha_1^2 & -4\,e_3^a\,\alpha_3 \\ -4\,e_3\,\alpha_3 & 2\,d_2 \end{bmatrix} \tag{20}$$

The final 2 × 2 mass squared matrix describes the kappa-type scalars (I=1/2, P=+):

$$\left(X_\kappa^2\right) = \begin{bmatrix} -4\,e_3^a\,\beta_1 - 2\,c_2 + 4\,c_4\,\alpha_1^2 + 4\,c_4^a\,\alpha_1\,\alpha_3 + 4\,c_4\,\alpha_3^2 & -4\,e_3^a\,\alpha_1 \\ -4\,e_3^a\,\alpha_1 & 2\,d_2 \end{bmatrix} \tag{21}$$

In the case of the I=0 scalars there are four particles which mix with each other; the squared mass matrix then takes the form:

$$\left(X_0^2\right) = \begin{bmatrix} 4\,e_3^a\,\beta_3 - 2\,c_2 + 12\,c_4^a\,\alpha_1^2 & 4\sqrt{2}\,e_3^a\,\beta_1 & 4\,e_3^a\,\alpha_3 & 4\sqrt{2}\,e_3^a\,\alpha_1 \\ 4\sqrt{2}\,e_3^a\,\beta_1 & -2\,c_2 + 12\,c_4^a\,\alpha_3^2 & 4\sqrt{2}\,e_3^a\,\alpha_1 & 0 \\ 4\,e_3^a\,\alpha_3 & 4\sqrt{2}\,e_3^a\,\alpha_1 & 2\,d_2 & 0 \\ 4\sqrt{2}\,e_3^a\,\alpha_1 & 0 & 0 & 2\,d_2 \end{bmatrix} \tag{22}$$

For this matrix the basis states are consecutively,

$$\begin{aligned} f_a &= \frac{S_1^1 + S_2^2}{\sqrt{2}} \qquad n\bar{n}, \\ f_b &= S_3^3 \qquad s\bar{s}, \\ f_c &= \frac{S_1'^1 + S_2'^2}{\sqrt{2}} \qquad ns\bar{n}\bar{s}, \\ f_d &= S_3'^3 \qquad nn\bar{n}\bar{n}. \end{aligned} \tag{23}$$

The non-strange (n) and strange (s) quark content for each basis state has been listed at the end of each line above.

In the case of the four I=0 pseudoscalars, the mixing matrix formula is a long one which is given in Appendix B.

IV. PARAMETERS AND SOME PREDICTIONS

A simplifying feature in the present model is that, as previously, the parameters other than c_3 and γ_1 may be found without considering the four I=0 pseudoscalars. This is due to the presence of "ln's" in the last two terms of

the potential, V_0. So we consider the initial (six) parameters first. In Appendix A, a method is presented for their consecutive determination in a convenient way.

Here we consider the strange to non-strange quark mass ratio, A_3/A_1 to be an input. For many years this has been known, from various analyses of the chiral treatment [36], of the light pseudoscalars, to be around 25. In Fig.1 the dependence of the predicted decay constant ratio F_K/F_π on the quark mass ratio, including the dependence on the parameter $m[\pi(1300)]$ is shown. For comparison, the experimental ratio [37] is $F_K/F_\pi \approx 1.19$. Thus, the model predictions are seen to be quite reasonable, although perhaps a bit too small for typical parameter choices. This ratio may be fine-tuned by including non-minimal kinetic terms in the Lagrangian. See e.g. Eq.(4.1) of [38].

It is interesting to compare the values of the Lagrangian coefficients of the fully chiral invariant terms, c_2, c_4^a, d_2, e_3^a as obtained here and displayed in Fig.2 with the corresponding ones obtained in the zero quark mass model: Fig.2 of [31]. These parameters are clearly substantially similar to those in the zero quark mass case. This is a comforting feature since it agrees with the expectation that the light quark masses make only small changes in the QCD dynamics.

On the lowest two rows of Fig.2 we display the variations with A_3/A_1 and m$[\pi(1300)]$ of the two-quark condensates, the four-quark condensates and the quark mass type quantities A_1 and A_3.

In Fig.3 we give the predictions for the masses of the strange mesons and the I=0 scalars, showing the variations due to choosing different values of m$[\pi(1300)]$ and A_3/A_1. It is seen that the mass of the ordinary kaon is better fit for A_3/A_1 closer to 30 than to 20. The predicted mass of the "excited" kaon is roughly similar to the (mentioned, but not established) candidate K(1460).

The upper, right graph of Fig.3 displays the two predicted kappa-type particle masses. These are roughly consistent with the (discussed in [36] but not established)$K_0^*(800)$ and the $K_0^*(1430)$. It should be mentioned that the masses obtained in this paper are being considered as "bare" ones, subject to non-trivial "renormalization" due to effects which provide unitarity corrections to the scattering amplitudes in which these particles appear as poles. This is illustrated for the single-M linear sigma model case in [19]. A similar remark applies to the particle widths obtained from the third derivatives of the potential.

The graphs in the bottom row of Fig.3 display the predicted masses of the four I=0 scalars. Clearly the lighter two can be identified with the $f_0(600)$[sigma] and the $f_0(980)$. Note that the very light sigma is an inevitable consequence of the present model and was not put in by hand. There are three candidates,$f_0(1370)$,$f_0(1500)$ and $f_0(1710)$[one of which may be a glueball], for the heavier two particles.

In Fig.4 the predicted decay constants (i.e. the coefficients of the single particle terms in the appropriate axial vector or vector Noether currents) for the π', the K, the K', the κ and the κ' are shown with their parameter dependences. Note that $F_{\pi'}$ is very small but not exactly zero. This causes, as discussed in [32], a very small violation of the "partially conserved" axial vector current ansatz in this kind of mixing model.

One of our chief concerns here is the percentage "content" of "two quarks" (i.e. the $q\bar{q}$ content) vs. the percentage content of "four quarks" predicted to be in each particle state. In Fig.5 these percentages are shown for the particles having non-zero isospin quantum number. For comparison with the SU(3) symmetric cases considered in [31] and [32], note that the typical value of $m[\pi(1300)]$ considered there was about 1215 MeV. Then we see that the ordinary pion has, as before, about a 15 percent 4-quark content (and 85 percent 2-quark content). The "excited" pion, $\pi(1300)$ is predicted to have an 85 percent 4-quark content in this picture. Similarly, we see that the ordinary kaon is predicted to have about a 14 percent 4-quark content while the "excited" kaon has about an 86 percent 4-quark content. Notably, as before, the situation is drastically different for the scalar states. We read off that the lighter I=1 scalar, $a_0(980)$ has about a 76 percent 4-quark content and the lighter kappa has about a 92 percent 4-quark content.

The more complicated situation of the four mixing I=0 scalars is described in Fig.6. To read this, first note that the four physical states are labelled f_1, f_2, f_3, f_4 in order of increasing mass. Each is a linear combination of the basis states f_a, f_b, f_c, f_d given in Eq.(23). f_a and f_b are 2-quark type while f_c and f_d are 4-quark type. Thus the lowest lying I=0 scalar, $f_1 \equiv \sigma$, taking A_3/A_1=30 and $m[\pi(1300)] = 1215$ MeV, has percentages in each basis state of,

$$0.36,\ 0.04,\ 0.36,\ 0.24. \tag{24}$$

Altogether the sigma is about 40 percent 2-quark and 60 percent 4-quark in this case. This is similar to the roughly 50-50 split we found in the SU(3) symmetric case (See Fig.2 of[32]). f_2, the next heaviest I=0 state is about 95 percent 4-quark and 5 percent 2-quark. The two heaviest I=0 scalars both have majority two quark nature: f_3 is read to be about 63 percent 2-quark while f_4 is read to be about 93 percent 2-quark.

V. I=0 PSEUDOSCALARS

The elements of the squared mass matrix for I=0 pseudoscalars (given in Appendix B) are quite complicated and as a result it is convenient to treat this sector separately. As previously discussed, in this case the squared mass matrix contains two additional parameters (c_3 and γ_1) that only contribute to the properties of the I=0 pseudoscalars. It is

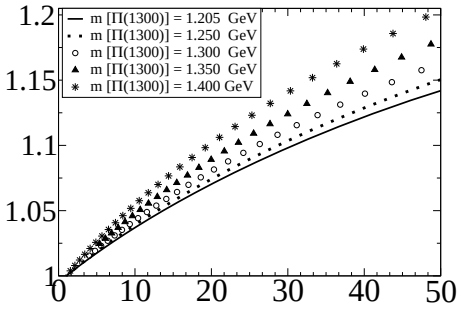

FIG. 1: $\frac{F_K}{F_\pi}$ vs $\frac{A_3}{A_1}$.

therefore not possible to trade these two parameters with four experimental η masses. Instead, we determine c_3 and γ_1 by fitting the trace and the determinant of the squared mass matrix to their corresponding experimental values, i.e. we solve for c_3 and γ_1 from the following equations:

$$\begin{aligned} \text{Tr}\,\left(M_\eta^2\right) &= \text{Tr}\,\left(M_\eta^2\right)_{\text{exp}} \\ \det\left(M_\eta^2\right) &= \det\left(M_\eta^2\right)_{\text{exp}} \end{aligned} \tag{25}$$

We identify the lighest two η's predicted by our model (i.e. η_1 and η_2) with $\eta(547)$ and $\eta'(958)$ with experimental masses [36]:

$$\begin{aligned} m^{\text{exp.}}[\eta(547)] &= 547.853 \pm 0.024\,\text{MeV}, \\ m^{\text{exp.}}[\eta'(958)] &= 957.66 \pm 0.24\,\text{MeV}. \end{aligned} \tag{26}$$

However, for the two heavier η's that our model predicts (i.e. η_3 and η_4) there are several experimental candidates below 2 GeV with masses [36]:

$$\begin{aligned} m^{\text{exp.}}[\eta(1295)] &= 1294 \pm 4\,\text{MeV}, \\ m^{\text{exp.}}[\eta(1405)] &= 1409.8 \pm 2.5\,\text{MeV}, \\ m^{\text{exp.}}[\eta(1475)] &= 1476 \pm 4\,\text{MeV}, \\ m^{\text{exp.}}[\eta(1760)] &= 1756 \pm 9\,\text{MeV}. \end{aligned} \tag{27}$$

We consider all six possible choices for identifying η_3 and η_4 with two of the above four experimental candidates. This leads to six scenarios given in table III. Equations (25) result in a quadratic equation for γ_1 for which the discriminant versus $m_\pi(1300)$ is plotted for all six scenarios in Fig. 7. We see that for $A_3/A_1 = 20$ the scenarios 1, 2 and 4 are completely ruled out, whereas for $A_3/A_1 = 30$ up to $m_\pi(1300) \approx 1.25$ GeV all six scenarios are possible.

Therefore, for a given scenario there are two solutions for γ_1 and c_3, and consequently two sets of predictions for the four η masses. We measure the goodness of each solution by the smallness of the following quantity:

$$\chi_{sl} = \sum_{k=1}^{4} \frac{\left|m_{sl}^{\text{theo.}}(\eta_k) - m_s^{\text{exp.}}(\eta_k)\right|}{m_s^{\text{exp.}}(\eta_k)} \tag{28}$$

in which s corresponds to the scenario (i.e. $s = 1 \cdots 6$) and l corresponds to the solution number (i.e. $l = 1, 2$). The quantity $\chi_{sl} \times 100$ gives the overall percent discrepancy between our theoretical prediction and experiment. For the six scenarios and the two solutions for each scenario, χ_{sl} is plotted versus $m_\pi(1300)$ in Fig. 8. Clearly, scenario 3 is favored over the range of $m_\pi(1300)$.

Here, we present our predictions for the best fitting scenario 3 with $A_3/A_1 = 30$. (Of course, the other scenarios with different values of A_3/A_1 may also be of some interest for a more detailed look at additional properties of the system of the four etas). In the present case, the η masses are shown in Fig. 9 and we can clearly see a reasonable range of masses: The first mass is around 550 MeV (consistent with identifying it with $\eta(547)$), the second mass is in the range of 970 - 986 MeV (consistent with identifying it with $\eta(985)$), the third mass is in the range of 1218 - 1250

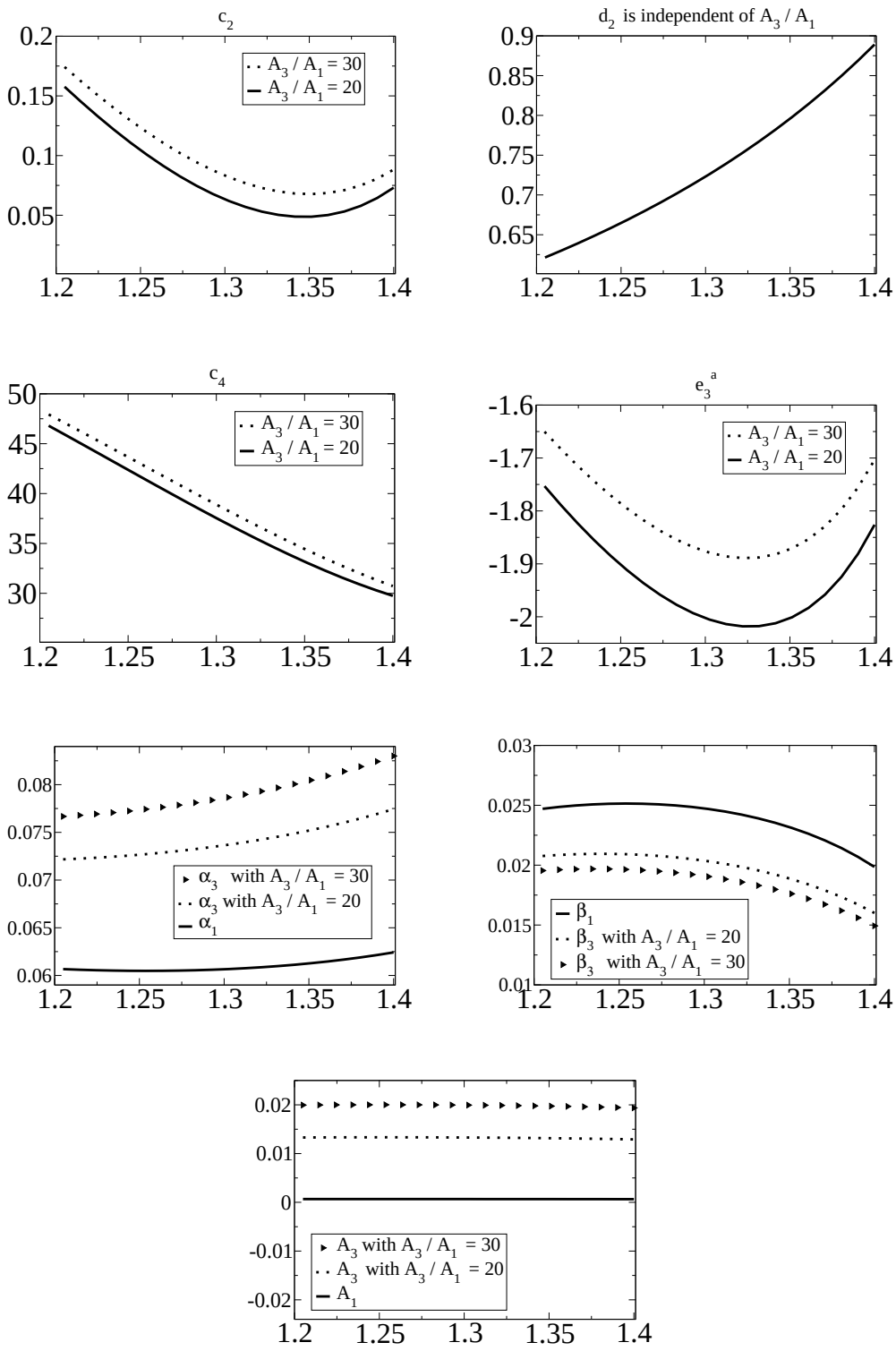

FIG. 2: Parameters vs $m[\pi(1300)]$ (GeV): c_2 (GeV^2) (top left), d_2 (GeV^2) (top right), c_4 (second row left), e_3 (GeV)(second row right), α_1 and α_3 (GeV)(third row left), β_1 and β_3 (GeV^2) (third row right) and A_1 and A_3 (GeV^3) (last row). (Note that d_2, α_1, β_1 and A_1 do not depend on the choice of $\frac{A_3}{A_1}$.)

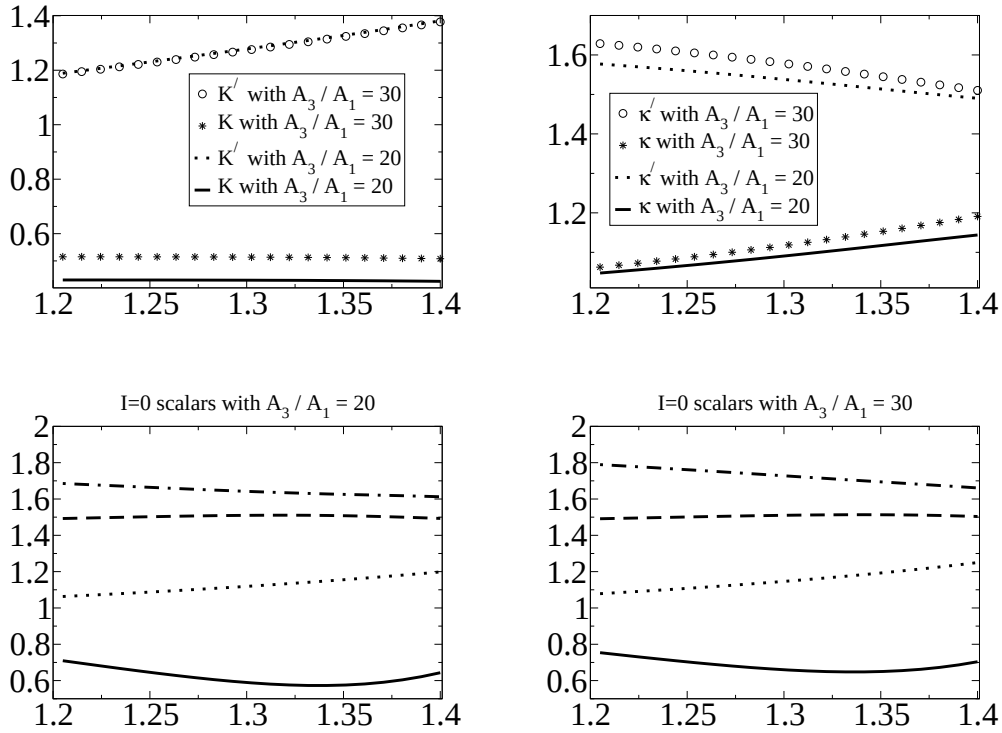

FIG. 3: Predicted masses (GeV) vs $m[\pi(1300)]$ (GeV): kaon system (top left), kappa system (top right), isoscalar salars (last row).

MeV (consistent with identifying it with $\eta(1295)$) and the fourth mass is around 1780 - 1790 MeV (consistent with identifying it with $\eta(1760)$).

The quark contents of the η's are given in Fig. 10 and show a clear difference compared to those of the I=0 scalars. The first two states ($\eta(547)$ and $\eta(985)$) are dominantly of two quark nature whereas the two heavier states ($\eta(1295)$ and $\eta(1760)$) are mainly four-quark states.

Scenario	η's
1	$\eta(547), \eta(958), \eta(1295), \eta(1405)$
2	$\eta(547), \eta(958), \eta(1295), \eta(1475)$
3	$\eta(547), \eta(958), \eta(1295), \eta(1760)$
4	$\eta(547), \eta(958), \eta(1405), \eta(1475)$
5	$\eta(547), \eta(958), \eta(1405), \eta(1760)$
6	$\eta(547), \eta(958), \eta(1475), \eta(1760)$

TABLE III: The six scenarios for identifying the predictions of our model for four ηs.

VI. CONCLUSIONS AND DISCUSSION

The results obtained [39] seem to provide support for the picture of light scalars having a predominant content of two quarks and two antiquarks while the heavier scalars appear to be made mainly from one quark and one antiquark, as one would expect from p wave states in the non relativistic quark model. The predicted scalar and pseudoscalar masses were seen to be reasonably consistent with the experimental candidates listed in [36].

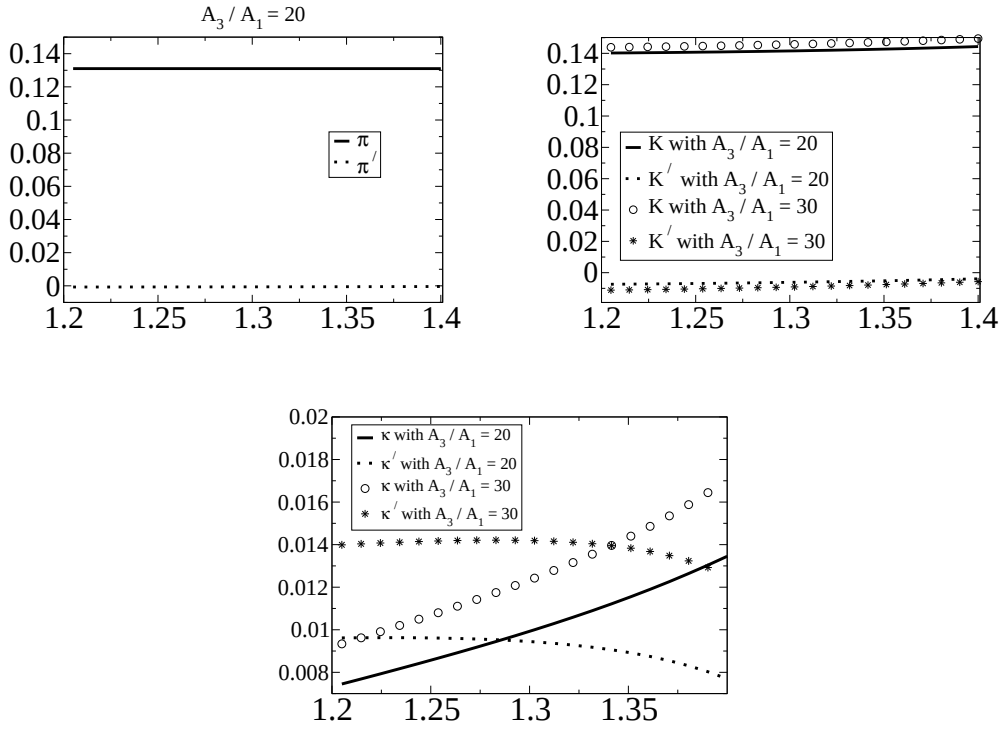

FIG. 4: Predicted decay constants (GeV) vs $m[\pi(1300)]$ (GeV): pion system (top left), kaon (top right), kappa system (last row). The result for pion system is insensitive to A_3/A_1.

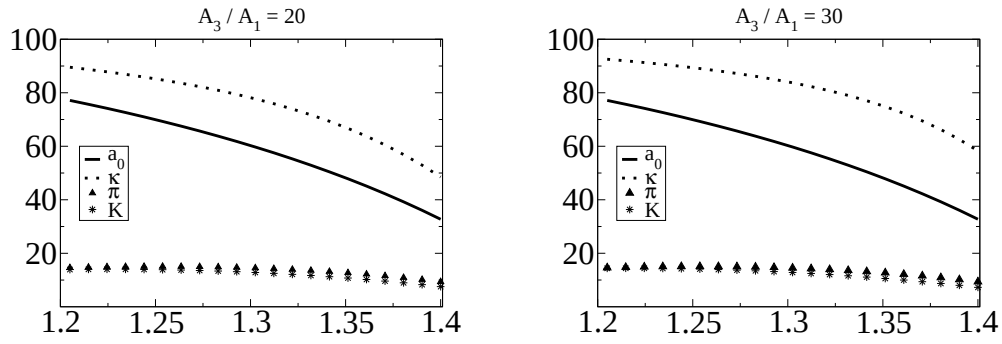

FIG. 5: Predicted percentage of four quark contents vs $m[\pi(1300)]$ (GeV).

While it appears a little unusual to think of say, the ordinary pion, as having some four quark content when treated in the effective Lagrangian framework, that is in fact the standard picture in the parton model approach to QCD. In the case of the two scalar nonets, the mass ordering itself naturally suggested such a picture. This picture was then inherited by the pseudoscalars when we chose to describe the scalars via a linear sigma model. There does not seem to be any problem with our treatment of the lighter pseudoscalar nonet. One might initially worry that the well established "current algebra" theorem for low energy pion pion scattering could get altered in the case of such a more complicated pion. However, we showed in [31] and [32] that there is only a small effect for this theorem. The situation concerning the heavier (mostly four quark) pseudoscalar nonet which appears in our model is neither so clear experimentally nor theoretically. Evidently this seems a fruitful direction for further investigation. The two

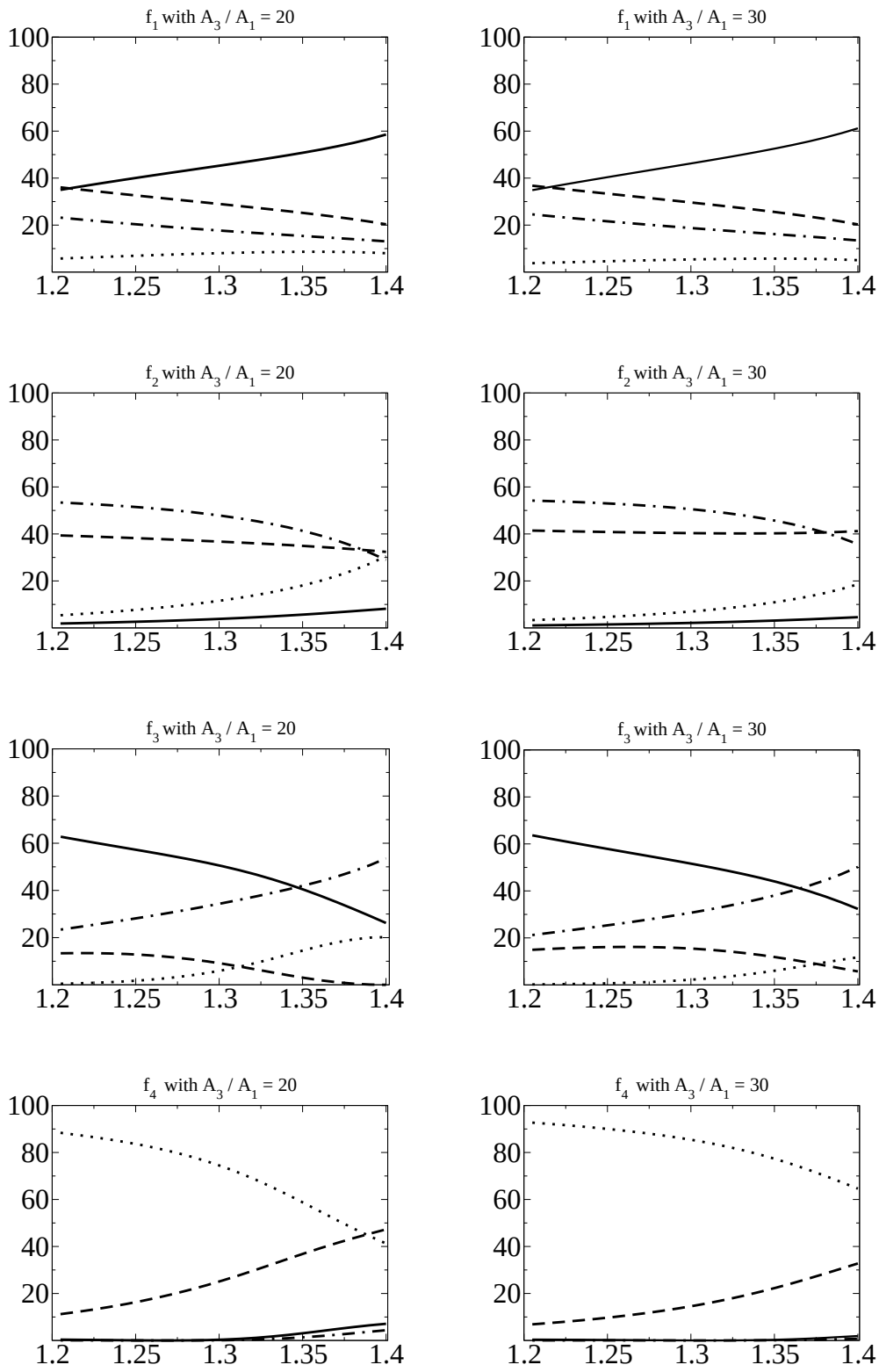

FIG. 6: Predicted quark contents of isoscalar scalar mesons vs $m[\pi(1300)]$ (GeV). The components [described in Eq. (23)] are: f_a (solid line), f_b (dotted line), f_c (dashed line) and f_d (dotted-dashed line).

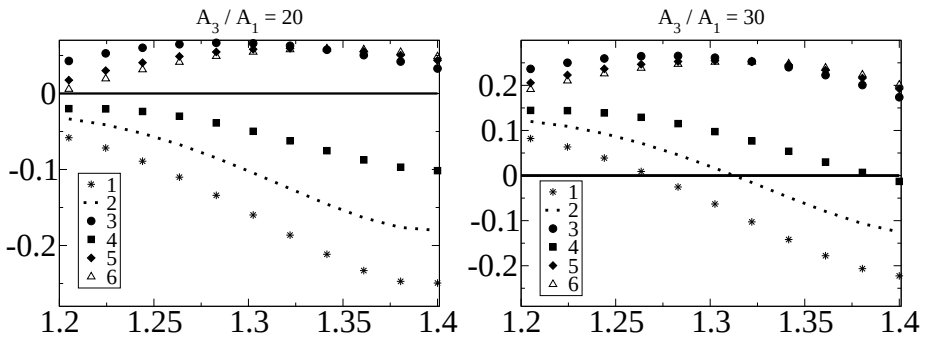

FIG. 7: Discriminant vs $m[\pi(1300)]$ (GeV).

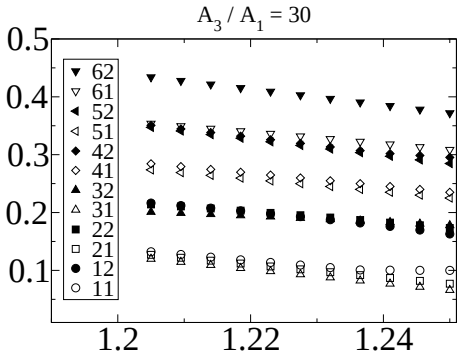

FIG. 8: χ_{sl} vs $m[\pi(1300)]$ (GeV).

new ηs which appear in this model are welcome from an experimental standpoint and the mixing with an expected glueball in this energy range is another interesting future topic. There is of course a similar glueball expected in the scalar isoscalar channel.

In addition to the "global" analysis of the mass spectrum and substructure presented here, the "local" topic of the detailed structure of the pion and kaon scattering is also of great interest. Recently progress has been made in this area, strongly supporting the existence of both the sigma and kappa mesons, by using ([27] and [40]) the chiral perturbation theory approach combined with some dispersion theory results [41]. Even though the present model is rather complicated, the fact that it is chiral symmetric means that we are guaranteed to get essentially the starting results of the chiral perturbation theory approach near the appropriate thresholds. In fact, since the light scalar fields are included, the starting results are even closer to the modern ones just mentioned. Thus we plan to next investigate the meson meson scattering scatterings in a number of different channels and at energies away from threshold. We are encouraged to go further by the results [19] obtained some time ago by unitarizing the scattering amplitudes computed using a single chiral SU(3) nonet model.

Actually, we have already started on this work and would like to briefly mention a result for the lowest lying scalar meson since it gives an idea of the accuracy to be expected for the masses we have presented in this paper. A more detailed analysis of the scattering amplitudes will be presented elsewhere.

The mass spectrum of the light scalars receives considerable unitarity corrections due to low-energy rescattering effects. The masses obtained above appear as tree level quantities in the effective Lagrangian under discussion. Especially in the case of the scalars the physical states are rather broad and will appear as poles in the scattering of two pseudoscalar mesons. A simple way to estimate the scattering amplitude is to first compute the tree level scalar partial wave scattering amplitude and then unitarize it by using the K-matrix method. This is equivalent to an earlier

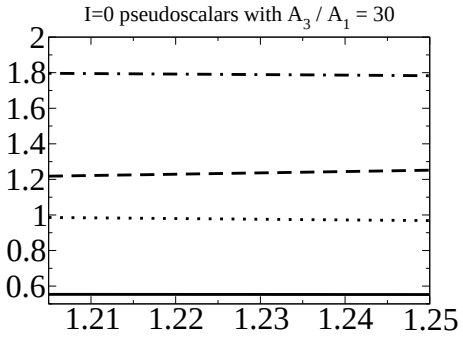

FIG. 9: Predicted η masses vs $m[\pi(1300)]$ (GeV).

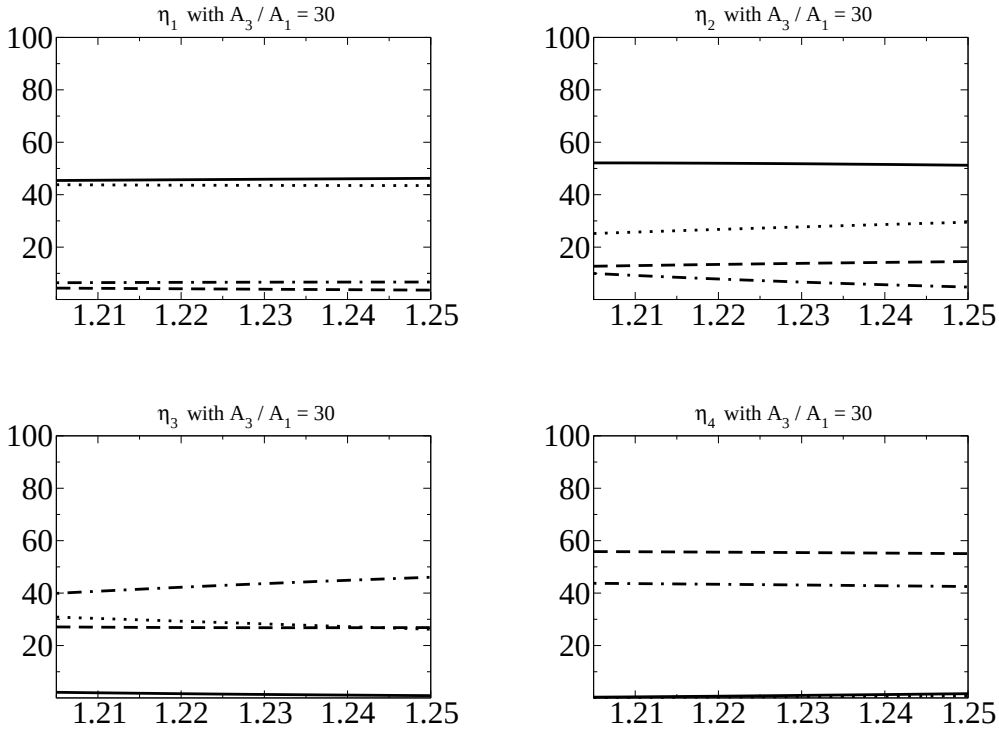

FIG. 10: Predicted quark contents of isoscalar pseudoscalar mesons vs $m[\pi(1300)]$ (GeV). The components [described in Eq. (B11)] are: η_a (solid line), η_b (dotted line), η_c (dashed line) and η_d (dotted-dashed line).

approach [4] and amounts to replacing the tree level amplitude, T_{tree} by,

$$T = \frac{T_{tree}}{1 - iT_{tree}}. \tag{29}$$

Following this procedure the sigma pole at 742 MeV discussed above appears in the unitarized pion scattering amplitude at $z \equiv M^2 - iM\Gamma$ with

$$M = 477\,\mathrm{MeV},\ \Gamma = 504\,\mathrm{MeV}. \tag{30}$$

This is of the same order as in [27]. Such scattering calculations should be performed to find the "actual" mass and width parameters for all the scalars in the present model.

Acknowledgments

We are happy to thank A. Abdel-Rehim, D. Black, M. Harada, S. Moussa, S. Nasri, N.W. Park, A.D. Polosa, F. Sannino and M.N. Shahid for many helpful related discussions. The work of A.H.F. has been partially supported by the NSF Award 0652853. The work of J.S. is supported in part by the U. S. DOE under Contract no. DE-FG-02-85ER 40231.

APPENDIX A: PARAMETER EVALUATION

By using the following formulas consecutively, it is possible to determine all the parameters of the model, one at a time, from the experimental inputs. The procedure is a more complicated version of the zero quark mass case given in Appendix B of [31] and the degenerate non-zero quark mass case given in the Appendix of [32].

We first use the I=1 scalar and pseudoscalar squared mass matrices to get the parameters,

$$\begin{aligned} 2d_2 &= \frac{m_a^2 m_{a'}^2 - m_\pi^2\, m_{\pi'}^2}{m_a^2 + m_{a'}^2 - m_\pi^2 - m_{\pi'}^2} \\ (\alpha_3\, e_3^a)^2 &= \frac{1}{64}((m_a^2 - m_{a'}^2)^2 - [4d_2 - (m_a^2 + m_{a'}^2)]^2) \end{aligned} \tag{A1}$$

The minimum equation then yields the ratio of the four quark to the two quark "condensate":

$$\frac{\beta_1}{\alpha_1} = -\frac{2(\alpha_3 e_3^a)}{d_2}. \tag{A2}$$

Next, the $\pi - \pi'$ mixing angle is found from the diagonalization of (M_π^2):

$$\cos 2\theta_\pi = \frac{4\, d_2 - m_\pi^2 - m_{\pi'}^2}{\sqrt{64\,(\alpha_3\, e_3^a)^2 + 16\, d_2^2 - 8\, d_2\,(m_\pi^2 + m_{\pi'}^2) + (m_\pi^2 + m_{\pi'}^2)^2}}. \tag{A3}$$

Then we get, from the formula for the pion decay constant [29],

$$\alpha_1 = \frac{1}{2}\,\frac{F_\pi}{\cos\theta_\pi - \left(\frac{\beta_1}{\alpha_1}\right)\,\sin\theta_\pi}, \tag{A4}$$

which then also gives β_1 using Eq.(A2) above.

To go beyond this point we introduce the strange to non-strange quark mass ratio, A_3/A_1 as an input parameter. We may then solve for the quantity $e_3^a\,\alpha_1$ by using the two minimum equations:

$$\begin{aligned} A_1 &= 2\,\beta_3\,(e_3^a\,\alpha_1) + 2\,\beta_1\,(e_3^a\,\alpha_3) - c_2\,\alpha_1 + 2\,c_4^a\,\alpha_1^3 \\ A_3 &= 4\,\beta_1\,(e_3^a\,\alpha_1) - c_2\,\alpha_3 + 2\,c_4^a\,\alpha_3^3 \end{aligned} \tag{A5}$$

Now, the rest of the parameters may be obtained by the consecutive use of the following equations:

$$\begin{aligned} c_4^a &= \frac{1}{8\,\alpha_1^2}\left[m_a^2 + m_{a'}^2 - m_\pi^2 - m_{\pi'}^2 - 16\,\frac{(\alpha_1\, e_3^a)^2}{d_2}\right] \\ 4\,c_2 &= 16\,\alpha_1^2\,c_4^a + 4\,d_2 - m_\pi^2 - m_{\pi'}^2 - m_a^2 - m_{a'}^2 \\ e_3^a &= \frac{(e_3^a\,\alpha_1)}{\alpha_1} \\ \alpha_3 &= \frac{(e_3^a\,\alpha_3)}{e_3^a} \\ \beta_3 &= \frac{\alpha_1\,\beta_1}{\alpha_3} \end{aligned}$$

$$
\begin{aligned}
(M_K^2)_{11} &= m_\pi^2 + m_{\pi'}^2 - 2\,d_2 + \frac{1}{2}\,(m_a^2 + m_{a'}^2 - m_\pi^2 - m_{\pi'}^2)\,\left(\frac{(e_3^a\,\alpha_3)^2}{(e_3^a\,\alpha_1)^2} - \frac{(e_3^a\,\alpha_3)}{(e_3^a\,\alpha_1)}\right) \\
&\quad -\frac{8}{d_2}\,\left[(\alpha_3\,e_3^a)^2 - (\alpha_1\,e_3^a)^2\right] \\
(M_K^2)_{12} &= -4\,(e_3^a\,\alpha_1) \\
(M_K^2)_{22} &= 2\,d_2 \\
\cos 2\theta_K &= \frac{(M_K^2)_{22} - (M_K^2)_{11}}{\sqrt{4\,(M_K^2)_{12}^2 + \left[(M_K^2)_{22} - (M_K^2)_{11}\right]^2}} \\
\frac{F_K}{F_\pi} &= \frac{\left(1 + \frac{(e_3^a\,\alpha_3)}{(e_3^a\,\alpha_1)}\right)\cos\theta_K - \frac{\beta_1}{\alpha_1}\left[1 + \frac{(e_3^a\,\alpha_1)}{(e_3^a\,\alpha_3)}\right]\sin\theta_K}{2\,\cos\theta_\pi - 2\,\left(\frac{\beta_1}{\alpha_1}\right)\sin\theta_\pi}
\end{aligned}
\tag{A6}
$$

With $m[\pi(1300)] = 1.215$ GeV and $A_3/A_1 = 30$, these parameters are given in table IV. In this case, the rotation matrices that related the flavor bases to the physical states are given in (A7) and (A8).

$c_2(\mathrm{GeV}^2)$	$1.62\ \times 10^{-1}$
$d_2(\mathrm{GeV}^2)$	$6.30\ \times 10^{-1}$
$e_3^a(\mathrm{GeV})$	-1.68
c_4^a	47.0
$\alpha_1(\mathrm{GeV})$	$6.06\ \times 10^{-2}$
$\alpha_3(\mathrm{GeV})$	$7.68\ \times 10^{-2}$
$\beta_1(\mathrm{GeV})$	$2.49\ \times 10^{-2}$
$\beta_3(\mathrm{GeV})$	$1.96\ \times 10^{-2}$
$A_1(\mathrm{GeV}^3)$	$6.66\ \times 10^{-4}$
$A_3(\mathrm{GeV}^3)$	$2.00\ \times 10^{-2}$

TABLE IV: Calculated Lagrangian parameters:c_2, d_2, e_3^a, c_4^a and vacuum values: α_1, α_3, β_1 and β_3, with $m[\pi(1300)] = 1.215$ GeV and $A_3/A_1 = 30$.

$$
(R_\pi^{-1}) = \begin{bmatrix} 0.923 & 0.385 \\ -0.385 & 0.923 \end{bmatrix}, \quad (R_K^{-1}) = \begin{bmatrix} 0.925 & 0.379 \\ -0.379 & 0.925 \end{bmatrix}, \quad (L_a^{-1}) = \begin{bmatrix} 0.493 & -0.870 \\ 0.870 & 0.493 \end{bmatrix}, \quad (L_\kappa^{-1}) = \begin{bmatrix} 0.284 & -0.959 \\ 0.959 & 0.284 \end{bmatrix}. \tag{A7}
$$

$$
(L_o^{-1}) = \begin{bmatrix} 0.601 & 0.199 & 0.600 & 0.489 \\ -0.107 & 0.189 & 0.643 & -0.735 \\ 0.790 & -0.050 & -0.391 & -0.470 \\ 0.062 & -0.960 & 0.272 & -0.019 \end{bmatrix} \tag{A8}
$$

APPENDIX B: M_η^2

The elements of the symmetric matrix M_η^2 are given by:

$$
\begin{aligned}
\left(M_\eta^2\right)_{11} &= \big(16\,c_4\,{\alpha_1}^6{\beta_1}^2 + 16\,c_4\,{\alpha_1}^5\alpha_3\,\beta_1\,\beta_3 + 4\,c_4\,{\alpha_1}^4{\alpha_3}^2{\beta_3}^2 - 16\,e_3\,{\alpha_1}^4{\beta_1}^2\beta_3 - 16\,e_3\,{\alpha_1}^3\alpha_3\,\beta_1\,{\beta_3}^2 \\
&\quad -4\,e_3\,{\alpha_1}^2{\alpha_3}^2{\beta_3}^3 - 8\,c_2\,{\alpha_1}^4{\beta_1}^2 - 8\,c_2\,{\alpha_1}^3\alpha_3\,\beta_1\,\beta_3 - 2\,c_2\,{\alpha_1}^2{\alpha_3}^2{\beta_3}^2 - 16\,c_3\,{\gamma_1}^2{\alpha_1}^2{\beta_1}^2 \\
&\quad -32\,c_3\,{\gamma_1}^2\alpha_1\,\alpha_3\,\beta_1\,\beta_3 - 16\,c_3\,{\gamma_1}^2{\alpha_3}^2{\beta_3}^2 - 32\,c_3\,\gamma_1\,{\alpha_1}^2{\beta_1}^2 - 32\,c_3\,\gamma_1\,\alpha_1\,\alpha_3\,\beta_1\,\beta_3 \\
&\quad -16\,c_3\,{\alpha_1}^2{\beta_1}^2\big) \,/\, \left(\left(2\,\alpha_1\,\beta_1 + \alpha_3\,\beta_3\right)^2\,{\alpha_1}^2\right)
\end{aligned}
\tag{B1}
$$

$$\left(M_\eta^2\right)_{12} = \Big(-4\sqrt{2}\left(4\,e_3\,{\alpha_1}^3\alpha_3\,{\beta_1}^3 + 4\,e_3\,{\alpha_1}^2{\alpha_3}^2{\beta_1}^2\beta_3 + e3\,\alpha_1\,{\alpha_3}^3\beta_1\,{\beta_3}^2 + 4\,c3\,{\gamma_1}^2{\alpha_1}^2{\beta_1}^2 + 4\,c_3\,{\gamma_1}^2\alpha_1\,\alpha_3\,\beta_1\,\beta_3 + 4\,c3\,\gamma_1\,{\alpha_1}^2{\beta_1}^2 + 2\,c_3\,\gamma_1\,\alpha_1\,\alpha_3\,\beta_1\,\beta_3 + 2\,c_3\,\gamma_1\,{\alpha_3}^2{\beta_3}^2 + 2\,c_3\,\alpha_1\,\alpha_3\,\beta_1\,\beta_3\right)\Big) / \left(\left(2\,\alpha_1\,\beta_1 + \alpha_3\,\beta_3\right)^2\alpha_1\,\alpha_3\right) \tag{B2}$$

$$\left(M_\eta^2\right)_{13} = \left(-16\,e_3\,{\alpha_1}^2\alpha_3\,{\beta_1}^2 - 16\,e_3\,\alpha_1\,{\alpha_3}^2\beta_1\,\beta_3 - 4\,e_3\,{\alpha_3}^3{\beta_3}^2 - 16\,c_3\,{\gamma_1}^2\alpha_1\,\beta_1 - 16\,c_3\,{\gamma_1}^2\alpha_3\,\beta_3 + 16\,c_3\,\gamma_1\,\alpha_3\,\beta_3 + 16\,c_3\,\alpha_1\,\beta_1\right) / \left(\left(2\,\alpha_1\,\beta_1 + \alpha_3\,\beta_3\right)^2\right) \tag{B3}$$

$$\left(M_\eta^2\right)_{14} = \Big(-4\sqrt{2}\left(4\,e_3\,{\alpha_1}^4{\beta_1}^2 + 4\,e_3\,{\alpha_1}^3\alpha_3\,\beta_1\,\beta_3 + e_3\,{\alpha_1}^2{\alpha_3}^2{\beta_3}^2 + 2\,c_3\,{\gamma_1}^2\alpha_1\,\alpha_3\,\beta_1 + 2\,c_3\,{\gamma_1}^2{\alpha_3}^2\beta_3 - 2\,c_3\,\gamma_1\,{\alpha_3}^2\beta_3 - 2\,c_3\,\alpha_1\,\alpha_3\,\beta_1\right)\Big) / \left(2\,\alpha_1\,\beta_1 + \alpha_3\,\beta_3\right)^2\alpha_1 \tag{B4}$$

$$\left(M_\eta^2\right)_{22} = \left(16\,c_4\,{\alpha_1}^2{\alpha_3}^4{\beta_1}^2 + 16\,c_4\,\alpha_1\,{\alpha_3}^5\beta_1\,\beta_3 + 4\,c_4\,{\alpha_3}^6{\beta_3}^2 - 8\,c_2\,{\alpha_1}^2{\alpha_3}^2{\beta_1}^2 - 8\,c_2\,\alpha_1\,{\alpha_3}^3\beta_1\,\beta_3 - 2\,c_2\,{\alpha_3}^4{\beta_3}^2 - 32\,c_3\,{\gamma_1}^2{\alpha_1}^2{\beta_1}^2 - 32\,c_3\,\gamma_1\,\alpha_1\,\alpha_3\,\beta_1\,\beta_3 - 8\,c_3\,{\alpha_3}^2{\beta_3}^2\right) / \left(\left(2\,\alpha_1\,\beta_1 + \alpha_3\,\beta_3\right)^2{\alpha_3}^2\right) \tag{B5}$$

$$\left(M_\eta^2\right)_{23} = \Big(-4\sqrt{2}\left(4\,e_3\,{\alpha_1}^2\alpha_3\,{\beta_1}^2 + 4\,e_3\,\alpha_1\,{\alpha_3}^2\beta_1\,\beta_3 + e_3\,{\alpha_3}^3{\beta_3}^2 + 4\,c_3\,{\gamma_1}^2\alpha_1\,\beta_1 - 4\,c_3\,\gamma_1\,\alpha_1\,\beta_1 + 2\,c_3\,\gamma_1\,\alpha_3\,\beta_3 - 2\,c_3\,\alpha_3\,\beta_3\right)\alpha_1\Big) / \left(\left(2\,\alpha_1\,\beta_1 + \alpha_3\,\beta_3\right)^2\alpha_3\right) \tag{B6}$$

$$\left(M_\eta^2\right)_{24} = \left(-8\,\left(\gamma_1 - 1\right)\left(2\,\gamma_1\,\alpha_1\,\beta_1 + \alpha_3\,\beta_3\right)c_3\right) / \left(2\,\alpha_1\,\beta_1 + \alpha_3\,\beta_3\right)^2 \tag{B7}$$

$$\left(M_\eta^2\right)_{33} = \left(8\,d_2\,{\alpha_1}^2{\beta_1}^2 + 8\,d_2\,\alpha_1\,\alpha_3\,\beta_1\,\beta_3 + 2\,d_2\,{\alpha_3}^2{\beta_3}^2 - 16\,c_3\,{\gamma_1}^2{\alpha_1}^2 + 32\,c_3\,\gamma_1\,{\alpha_1}^2 - 16\,c_3\,{\alpha_1}^2\right) / \left(2\,\alpha_1\,\beta_1 + \alpha_3\,\beta_3\right)^2 \tag{B8}$$

$$\left(M_\eta^2\right)_{34} = \left(-8\,\left(\gamma_1 - 1\right)^2\sqrt{2}c_3\,\alpha_1\,\alpha_3\right) / \left(2\,\alpha_1\,\beta_1 + \alpha_3\,\beta_3\right)^2 \tag{B9}$$

$$\left(M_\eta^2\right)_{44} = \left(8\,d_2\,{\alpha_1}^2{\beta_1}^2 + 8\,d_2\,\alpha_1\,\alpha_3\,\beta_1\,\beta_3 + 2\,d_2\,{\alpha_3}^2{\beta_3}^2 - 8\,c_3\,{\gamma_1}^2{\alpha_3}^2 + 16\,c_3\,\gamma_1\,{\alpha_3}^2 - 8\,c_3\,{\alpha_3}^2\right) / \left(2\,\alpha_1\,\beta_1 + \alpha_3\,\beta_3\right)^2 \tag{B10}$$

The basis states for the above matrix are:

$$\begin{aligned}
\eta_a &= \frac{\phi_1^1 + \phi_2^2}{\sqrt{2}},\\
\eta_b &= \phi_3^3,\\
\eta_c &= \frac{\phi_1'^1 + \phi_2'^2}{\sqrt{2}},\\
\eta_d &= \phi_3'^3.
\end{aligned} \tag{B11}$$

$c_3(\mathrm{GeV}^4)$	-3.78×10^{-4}
γ_1	5.27×10^{-3}

TABLE V: Calculated parameters: c_3 and γ_1.

With $m[\pi(1300)] = 1.215$ GeV and $A_3/A_1 = 30$, these paprameters are given in table V.
In this case, the rotation matrix for I=0 pseudoscalars becomes:

$$(R_o^{-1}) = \begin{bmatrix} -0.675 & 0.661 & -0.205 & 0.255 \\ 0.722 & 0.512 & -0.363 & 0.291 \\ -0.134 & -0.546 & -0.519 & 0.644 \\ 0.073 & 0.051 & 0.746 & 0.660 \end{bmatrix} \tag{B12}$$

[1] E. van Beveren, T.A. Rijken, K. Metzger, C. Dullemond, G. Rupp and J.E. Ribeiro, Z. Phys. **C30**, 615 (1986).
[2] D. Morgan and M. Pennington, Phys. Rev. **D48**, 1185 (1993).
[3] A.A. Bolokhov, A.N. Manashov, M.V. Polyakov and V.V. Vereshagin, Phys. Rev. **D48**, 3090 (1993).
[4] N.N. Achasov and G.N. Shestakov, Phys. Rev. **D49**, 5779 (1994). A summary of the recent work of the Novosibirsk group is given in N.N. Achasov, arXiv:0810.2601[hep-ph].
[5] R. Kamínski, L. Leśniak and J. P. Maillet, Phys. Rev. **D50**, 3145 (1994).
[6] F. Sannino and J. Schechter, Phys. Rev. **D52**, 96 (1995).
[7] G. Janssen, B.C. Pearce, K. Holinde and J. Speth, Phys. Rev. **D52**, 2690 (1995).
[8] R. Delbourgo and M.D. Scadron, Mod. Phys. Lett. **A10**, 251 (1995).
[9] N.A. Törnqvist and M. Roos, Phys. Rev. Lett. **76**, 1575 (1996).
[10] M. Svec, Phys. Rev. **D53**, 2343 (1996).
[11] S. Ishida, M.Y. Ishida, H. Takahashi, T. Ishida, K. Takamatsu and T Tsuru, Prog. Theor. Phys. **95**, 745 (1996).
[12] M. Harada, F. Sannino and J. Schechter, Phys. Rev. **D54**, 1991 (1996).
[13] A.V. Anisovich and A.V. Sarantsev, Phys. Lett. **B413**, 137 (1997).
[14] D. Black, A.H. Fariborz, F. Sannino and J. Schechter, Phys. Rev. **D58**, 054012 (1998).
[15] J.A. Oller, E. Oset and J.R. Pelaez, Phys. Rev. Lett. **80**, 3452 (1998).
[16] V. Elias, A.H. Fariborz, Fang Shi and T.G. Steele, Nucl. Phys. **A633**, 279 (1998).
[17] K. Igi and K. Hikasa, Phys. Rev. **D59**, 034005 (1999).
[18] D. Black, A.H. Fariborz, F. Sannino and J. Schechter, Phys. Rev. **D59**, 074026 (1999).
[19] D. Black, A.H. Fariborz, S. Moussa, S. Nasri and J. Schechter, Phys. Rev. D **64**, 014031 (2001).
[20] R.L. Jaffe, Phys. Rev. D **15**, 267 (1977).
[21] J.D. Weinstein and N. Isgur, Phys. Rev. Lett. **48**, 659 (1982).
[22] D. Black, A. H. Fariborz and J. Schechter, Phys. Rev. D **61** 074001 (2000).
[23] T. Teshima, I. Kitamura and N. Morisita, J. Phys. G **28**, 1391 (2002); *ibid* **30**, 663 (2004); F. Close and N. Tornqvist, *ibid.* **28**, R249 (2002); A.H. Fariborz, Int. J. Mod. Phys. A **19**, 2095 (2004); 5417 (2004); Phys. Rev. D **74**, 054030 (2006);
[24] M. Napsuciale and S. Rodriguez, Phys. Rev. D **70**, 094043 (2004); F. Giacosa, Th. Gutsche, V.E. Lyubovitskij and A. Faessler, Phys. Lett. B **622**, 277 (2005); J. Vijande, A. Valcarce, F. Fernandez and B. Silvestre-Brac, Phys. Rev. D **72**, 034025 (2005); S. Narison, Phys. Rev. D **73**, 114024 (2006); L. Maiani, F. Piccinini, A.D. Polosa and V. Riquer, hep-ph/0604018; J.R. Pelaez, Phys. Rev. Lett. **92**, 102001 (2004); J.R. Pelaez and G. Rios, Phys. Rev. Lett. **97**, 242002 (2006); F. Giacosa, Phys. Rev. D **75**,054007 (2007).
[25] G. 't Hooft, G. Isidori, L. Maiani, A.D. Polosa and V. Riquer, arXiv:0801.2288[hep-ph].
[26] Related models for thermodynamic properties of QCD are N. Yamamoto, M. Tachibana, T. Hatsuda and G. Baym, Phys. Rev. D **76**, 074001 (2007) and A.A. Andrianov and D. Espriu, arXiv:0709.0049 [hep-ph].
[27] I. Caprini, G. Colangelo and H. Leutwyler, Phys. Rev. Lett. **96**, 132001 (2006).
[28] See section V of [19] above.
[29] A.H. Fariborz, R. Jora and J. Schechter, Phys. Rev. D **72**, 034001 (2005).
[30] A.H. Fariborz, R. Jora and J. Schechter, Phys. Rev. D **76**, 014011 (2007).
[31] A.H. Fariborz, R. Jora and J. Schechter, Phys. Rev. D **77**, 034006 (2008), arXiv:0707.0843 [hep-ph]. Note that some corrections to [29] above are given in Appendix A of this reference.
[32] A.H. Fariborz, R. Jora and J. Schechter, Phys. Rev. D **76**, 114001 (2007), arXiv:0708.3402 [hep-ph].
[33] A.H. Fariborz, R. Jora and J. Schechter, Phys. Rev. D **77**,094004 (2008), arXiv:0801.2552[hep-ph]. Related papers include E. Meggiolaro, Z. Phys. C **62**, 669 (1994) and [25] above.
[34] S. Weinberg, Phys. Rev. Lett.**17**, 616 (1966).
[35] The isospin violation case for the single-M linear sigma model was treated in J. Schechter and Y. Ueda, Phys. Rev. D **4**, 733 (1971).

[36] Review of Particle Physics, C. Amsler et al Phys. Lett. **B 667**, 1 (2008). See p.551 for this first citation.
[37] See p.820 of [36].
[38] H.Gomm, P.Jain, R.Johnson and J.Schechter, Phys. Rev. D **33**, 801 (1986).
[39] A preliminary announcement of some of these results was given in A.H. Fariborz, R. Jora and J. Schechter, QCD08 Montpellier conference proceedings, arXiv:0810.4640[hep-ph].
[40] S. Descotes-Genon and B. Moussallam, Eur. Phys. J. C **48**,553 (2006).
[41] S.M. Roy, Phys. Lett. **36B**, 353 (1971). See also D.V. Bugg, J. Phys. G **34**, 151 (2007).